

### 3D imaging of gravity gradiometry data from a single borehole using potential field migration

Xiaojun Liu\*, University of Utah, and Michael S. Zhdanov, University of Utah and TechnoImaging

#### Summary

We present a feasibility study for the rapid 3D imaging of borehole gravity gradiometry data. Our method is based on potential field migration, a method that enables us to recover a 3D density model around a single borehole by using a stable integral transform of the observed gravity gradients. The rapidity of the method means it can be used for real-time imaging, or for producing an a priori model for subsequent regularized inversion. Since borehole gravity gradiometers are still in development, we are at liberty to analyze imaging based on different components of the gravity tensor. The results of our feasibility study demonstrate the directional sensitivities of the gravity gradients, and show how potential migration can recover the location of bodies from both single and multiple gravity gradient measurements. However, some gravity tensor components measured from a single borehole are not sufficient to exactly recover the azimuth of a target nor to resolve multiple compact bodies.

#### Introduction

Borehole gravimetry is a bulk in-situ density logging method suggested as early as Smith (1950). In recent years, there has been a steady but building interest in borehole gravity surveying for both mining and hydrocarbon production where high density contrasts are expected, e.g., water flooding with a gas/water contact (Brady et al., 2006), gas injection into a heavy oil reservoir, CO<sub>2</sub> sequestration (Sherlock et al., 2006), and ore body delineation (Nind et al., 2007). For the past 40 years, industry practice has been to difference two gravity observations vertically separated in a borehole to derive an apparent density,  $\rho_a$ :

$$\rho_a = \frac{\Delta g_z}{4\pi\gamma h}, \quad (1)$$

where  $\gamma$  is the universal gravitational constant, and  $\Delta g_z$  is the difference in the vertical gravity field between two measurements separated by a vertical distance,  $h$ . Apparent density (1) is equal to the formation bulk density when the instrument passes vertically through beds which are horizontal, infinitely extended laterally, uniformly thick, and constant in density. In some instances, departures from these assumed conditions are so slight that their effects can be ignored, and borehole gravimetry essentially yields the bulk density with a large radius of investigation around the borehole (e.g., LaFehr, 1983). Given the aforementioned restrictions on borehole verticality and the radial symmetry of the vertical gravity field (i.e., lack of directional sensitivity), these horizontally layered interpretations were, for the most part, valid.

Limitations in existing instruments and renewed interest in borehole gravimetry for both hydrocarbon and mining applications have spurred the development of new BHGM instruments. Scintrex's Gravilog can be deployed in BQ boreholes and NQ drill rods up to deviations 60 degrees from vertical (Nind et al., 2007). Schlumberger's re-engineering of Gravilog under license from Scintrex will enable the instrument to enter boreholes of any orientation. The advantages of measuring gravity gradients rather than the gravity field have also been recognized (e.g., Nekut, 1989), and prototype borehole gravity gradiometers have since been developed by Gravitec (e.g., Golden et al., 2007) and Lockheed Martin (DiFrancesco, pers. comms.). 3D quantitative interpretations are required for gravity gradient measurements in deviated boreholes (e.g., Rim and Li, 2010), for survey designs including multiple boreholes (e.g., Kreiger et al., 2009), and for surface gravity measurements (e.g., Krahenbuhl and Li, 2008). Previous authors have presented 3D inversion as the basis of their quantitative interpretations. In the current paper, we develop an alternative approach based on 3D potential field migration as originally introduced by Zhdanov (2002), and subsequently developed for gravity gradiometry by Zhdanov et al. (2010). Since borehole gravity gradiometers are still being developed, we are at a liberty to analyze imaging based on different components. As we shall discuss, the advantage of migration over inversion is that it opens the possibility for real-time imaging for logging-while-drilling.

#### 3D migration imaging of the borehole gravity gradient fields

According to the principals of the potential field migration (Zhdanov, 2002; Zhdanov et al., 2010), the migration gravity tensor field,  $g_{\alpha\beta}^m(\mathbf{r})$ , is introduced as a result of application of the adjoint operator,  $A_{\alpha\beta}^*$ , to the observed gravity tensor field:

$$g_{\alpha\beta}^m(\mathbf{r}) = A_{\alpha\beta}^* g_{\alpha\beta}, \quad (2)$$

where  $g_{\alpha\beta}(\mathbf{r})$  are the second spatial derivatives of the gravity potential, and the corresponding adjoint operator,  $A_{\alpha\beta}^*$ , applied to some function,  $f(\mathbf{r})$ , is given by following expression:

$$A_{\alpha\beta}^*(f) = \int_L \frac{f(\mathbf{r}')}{|\mathbf{r}' - \mathbf{r}|^3} K_{\alpha\beta}(\mathbf{r}' - \mathbf{r}) d\mathbf{l}, \quad (3)$$

and the kernels  $K_{\alpha\beta}$  are equal to:

### 3D imaging of gravity gradiometry data from a single borehole using potential field migration

$$K_{\alpha\beta}(\mathbf{r}' - \mathbf{r}) = \begin{cases} 3 \frac{(\alpha - \alpha')(\beta - \beta')}{|\mathbf{r}' - \mathbf{r}|^2}, & \alpha \neq \beta \\ 3 \frac{(\alpha - \alpha')^2}{|\mathbf{r}' - \mathbf{r}|^2} - 1, & \alpha = \beta \end{cases}, \alpha, \beta = x, y, z.$$

A migration density can be determined by the following formula:

$$\rho_{\alpha\beta}^m(\mathbf{r}) = k_{\alpha\beta} w_{\alpha\beta}^{-2} g_{\alpha\beta}^m(\mathbf{r}), \quad \alpha, \beta = x, y, z, \quad (4)$$

where unknown coefficient  $k_{\alpha\beta}$  is determined by a linear line search (Zhdanov, 2002), and the linear weighting function,  $w_{\alpha\beta}$ , is equal to the square root of the integrated sensitivity of the gravity tensor field,  $S_{\alpha\beta}$ :

$$w_{\alpha\beta} = \sqrt{S_{\alpha\beta}}. \quad (5)$$

The integrated sensitivity  $S_{\alpha\beta}$ , in accordance with the definition, is calculated by the following formula:

$$S_{\alpha\beta} = \frac{\|\delta g_{\alpha\beta}^{obs}\|_G}{\delta\rho}, \quad (6)$$

where  $\delta g_{\alpha\beta}^{obs}$  is the perturbation of the gravity tensor field resulting from a local perturbation of the density,  $\delta\rho(\mathbf{r}') = \rho(\mathbf{r}')dV'$ , located at the point  $\mathbf{r}' = (x', y', z')$ . According to equation (4), the migration density is proportional to the magnitude of the weighted tensor migration field,  $g_{\alpha\beta}^m$ :

$$g_{\alpha\beta}^m(\mathbf{r}) = \int_L \frac{g_{\alpha\beta}(\mathbf{r}')}{|\mathbf{r}' - \mathbf{r}|^3} K_{\alpha\beta}(\mathbf{r}' - \mathbf{r}) dV'. \quad (7)$$

Finally, we can write the following expressions for the migration densities for the different gravity gradients as measured from a single borehole:

$$\rho_{\alpha\beta}^m(\mathbf{r}) = k_{\alpha\beta} w_{\alpha\beta}^{-2} \int_L \frac{g_{\alpha\beta}(\mathbf{r}')}{|\mathbf{r}' - \mathbf{r}|^3} K_{\alpha\beta}(\mathbf{r}' - \mathbf{r}) dV'. \quad (8)$$

#### Model study

In this section, we present three model studies for the potential field migration of gravity gradiometry data from a single borehole. In the first model study, we consider a single cubic body of 40 m dimension and 1 g/cm<sup>3</sup> density contrast located 40 m from the borehole (Figure 1). Figure 2 shows the observed data for different gravity gradients measured along the borehole trajectory. Note that the  $g_{xy}$  and  $g_{yz}$  data are effectively zero given machine precision. Figure 3 shows a vertical cross section in the x direction of the potential field migration results for the  $g_{zx}$ ,  $g_{zz}$ , and  $g_{\Delta}$  components, and the combined  $g_{\Delta}$  and  $g_{zx}$  components. One can clearly see in this map the correct locations of the body, which are the sources of the observed gravity gradients. The images on the left side of the borehole are

artificial, for we imaged with just one component; i.e., there was no radial symmetry. As expected, the migration of just the  $g_{zz}$  component shows a symmetrical density. From the migration of both  $g_{\Delta}$  and  $g_{zx}$  components, we have directional sensitivity and can see how the artificial source disappears.

Next, we investigate the directional sensitivity of different gravity gradient components. Figure 4 shows a horizontal cross section of the migration results for the independent  $g_{zz}$ ,  $g_{zx}$ , and  $g_{\Delta}$  components and the joint  $g_{\Delta}$  and  $g_{zx}$  components. We can see that the  $g_{zz}$  component recovers only the distance to the body but not the direction to the body. Migration of either the  $g_{zx}$  or the  $g_{\Delta}$  components recovers the correct location of the body, but the models are symmetric; i.e., one of the bodies is artificial. The joint migration of the  $g_{\Delta}$  and  $g_{zx}$  components recovers just a single body.

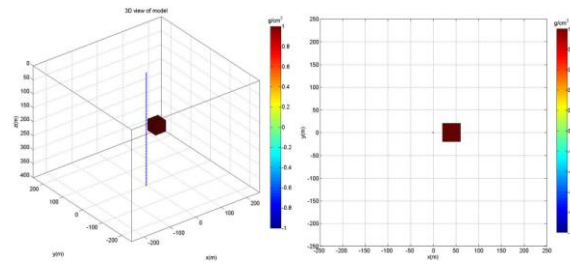


**Figure 1.** 3D perspective view (left panel) and plane view (right panel).

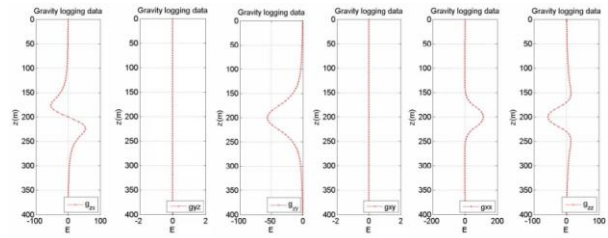


**Figure 2.** Simulated borehole gravity data single for a single cubic body of 40 m dimension and 1 g/cm<sup>3</sup> located 40 m from the borehole.

### 3D imaging of gravity gradiometry data from a single borehole using potential field migration

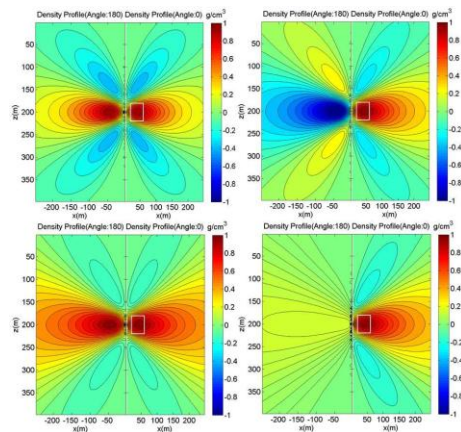


**Figure 3.** Vertical cross sections of 3D potential field migration of single and combinations of gravity gradient components: left top,  $g_{zz}$ ; right top,  $g_{zx}$ ; left bottom,  $g_{\Delta}$ ; right bottom,  $g_{\Delta}$  and  $g_{zx}$ .

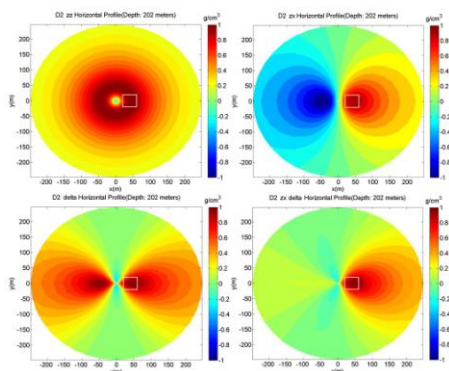


**Figure 4.** Horizontal cross sections of 3D potential field migration of single and combinations of gravity gradient components: left top,  $g_{zz}$ ; right top,  $g_{zx}$ ; left bottom,  $g_{\Delta}$ ; right bottom,  $g_{\Delta}$  and  $g_{zx}$ .

For the second model, we have investigated a faulted reservoir of  $-1 \text{ g/cm}^3$  density contrast (Figure 5). Figure 6 shows the observed data for different gravity gradients measured along the borehole trajectory. Figure 7 shows vertical cross sections of the potential field migration result in the  $x$  direction for the combined  $g_{\Delta}$  and  $g_{zx}$  components. We can see that from the migration of both the  $g_{\Delta}$  and  $g_{zx}$  components, we accurately recover the vertical location of the reservoirs.

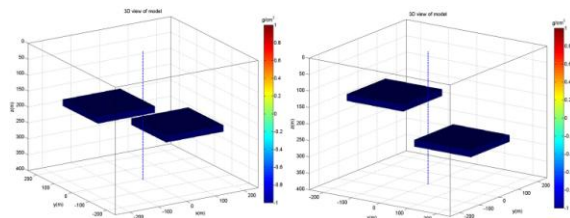


**Figure 5.** 3D perspective views of the faulted reservoir of  $-1 \text{ g/cm}^3$  density contrast.

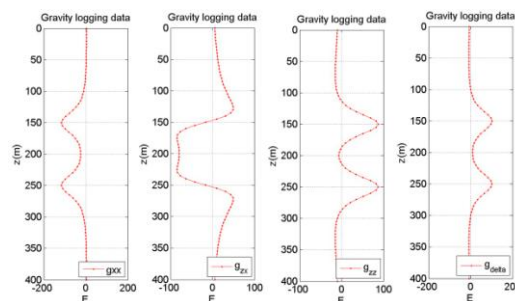


**Figure 6.** Simulated single borehole gravity data for the faulted reservoir of  $-1 \text{ g/cm}^3$  density contrast.

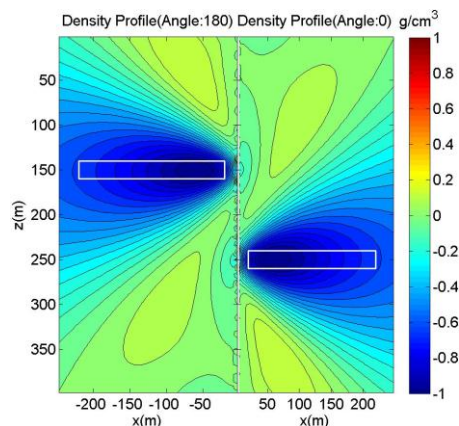


**Figure 7.** Vertical cross section of density obtained from joint migration of both  $g_{zx}$  and  $g_{\Delta}$  data.

### 3D imaging of gravity gradiometry data from a single borehole using potential field migration

For the third model, we again consider a single body. Our purpose is to test the resolution in order to locate the body's azimuth. We use two components,  $g_{zx}$  and  $g_{zy}$ , so as to emulate Gravitec's borehole gravity gradiometer. The body is a cube of 20 m dimension with a density contrast of  $-1 \text{ g/cm}^3$ . Figure 8 shows the migration result for the single components,  $g_{zx}$  and  $g_{zy}$ . We can see that it is difficult to identify the location of the body using a single component. At the same time, as shown in Figure 8, we observe that joint migration of both  $g_{zx}$  and  $g_{zy}$  components recover the correct direction of body. However, an artificial density distribution of equal amplitude but opposite sign exists. As such, we conclude that the,  $g_{zx}$  and  $g_{zy}$  components alone are not sufficient to reliably recover the 3D density models.

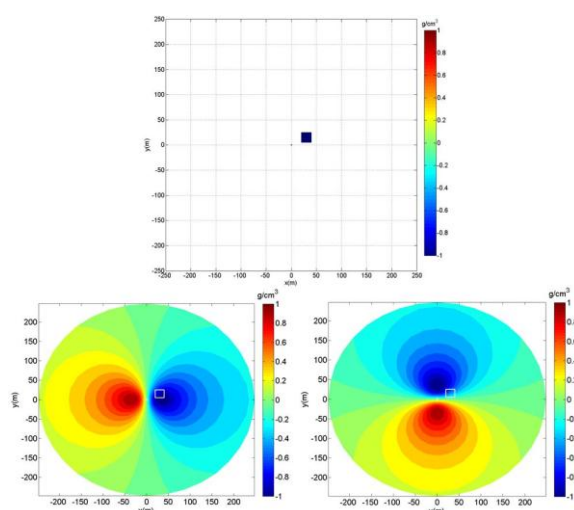


**Figure 8.** Plane view of the model and horizontal cross sections of the migration results for the,  $g_{zx}$  (left) and  $g_{zy}$  (right) components only.

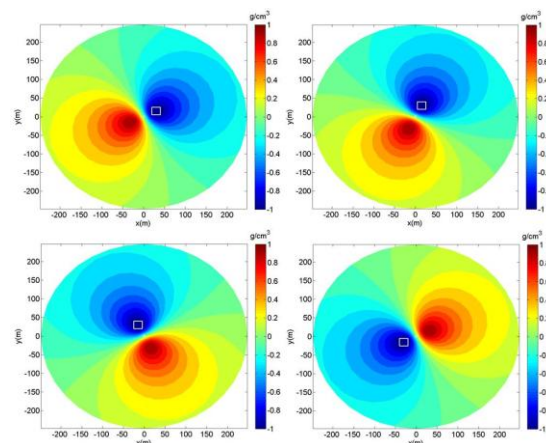


**Figure 9.** Horizontal cross sections of joint migration results for both the  $g_{zx}$  and  $g_{zy}$  components for different locations of the body.

### Conclusions

Potential field migration has been shown feasible for rapid 3D imaging of gravity gradiometry data measured from a single borehole. Our results suggest that migration of just a single component is insufficient to accurately image 3D targets, for example, to resolve azimuth and/or multiple compact bodies. Joint migration of at least two components is required to accurately image 3D targets. However, care must be given to which components are measured and interpreted. For example, our study suggests joint migration of both the,  $g_{zx}$  and  $g_{zy}$  components still produces inadequate images. Further research to identify which components are most suitable for realistic geologic targets (e.g., water flooding in hydrocarbon reservoirs) is warranted.

### Acknowledgements

The authors acknowledge the support of the University of Utah's Consortium for Electromagnetic Modeling and Inversion (CEMI) and TechnoImaging.



## EDITED REFERENCES

Note: This reference list is a copy-edited version of the reference list submitted by the author. Reference lists for the 2011 SEG Technical Program Expanded Abstracts have been copy edited so that references provided with the online metadata for each paper will achieve a high degree of linking to cited sources that appear on the Web.

## REFERENCES

- Brady, J. L., J. L. Hare, J. F. Ferguson, J. E. Seibert, F. J. Klopping, T. Chen, and T. Niebauer, 2006, Results of the world's first 4D microgravity surveillance of a waterflood – Prudhoe Bay, Alaska: Presented at Annual Technical Conference and Exhibition, SPE, doi: 10.2118/101762-MS.
- Golden, H., W. McRae, and A. Veryaskin, 2007, Description of and results from a novel borehole gravity gradiometer: Presented at 19th Geophysical Conference and Exhibition, ASEG.
- Krahenbuhl, R., and Y. Li, 2008, Joint inversion of surface and borehole 4D gravity data for continuous characterization of fluid contact movement: 78th Annual International Meeting, SEG, Expanded Abstracts, 726–729.
- Krieger, M., P. Smilde, and O. Geisler, 2009, Completing the image with borehole gravity gradients: 79th Annual International Meeting, SEG, Expanded Abstracts, 923–926.
- LaFehr, T. R., 1983, Rock density from borehole gravity surveys: *Geophysics*, **48**, 341–356.
- Nekut, A. G., 1989, Borehole gravity gradiometry: *Geophysics*, **54**, no. 2, 225–234, [doi:10.1190/1.1442646](https://doi.org/10.1190/1.1442646).
- Nind, C., H. O. Seigel, M. Chouteau, and B. Giroux, 2007, Development of a borehole gravimeter for mining applications: *First Break*, **25**, 71–77.
- Rim, H., and Y. Li, 2010, Single-borehole imaging using gravity gradiometer data: 80th Annual International Meeting, SEG, Expanded Abstracts, 1137–1140.
- Sherlock, D., A. Toomey, M. Hoversten, E. Gasperikova, and K. Dodds, 2006, Gravity monitoring of CO<sub>2</sub> storage in a depleted gas field: A sensitivity study: *Exploration Geophysics*, **37**, 37–43.
- Smith, N. J., 1950, The case for gravity data from boreholes: *Geophysics*, **15**, 605–636.
- Zhdanov, M. S., 2002, *Geophysical inverse theory and regularization problems*: Elsevier.
- Zhdanov, M. S., X. Liu, and G. Wilson, 2010, Potential field migration for rapid 3D imaging of gravity gradiometry surveys: *First Break*, **28**, no. 11, 47–51.